Journal of Alloys and Compounds 509 (2011) 7349–7355

Contents lists available at ScienceDirect

Journal of Alloys and Compounds

journal homepage: www.elsevier.com/locate/jallcom

Effect of Ce on solidification and mechanical properties of A360 alloy

Maja Vončina*, Stanislav Kores, Primož Mrvar, Jožef Medved

University of Ljubljana, Faculty of Natural Sciences and Engineering, Department of Materials and Metallurgy, Aškerčeva 12, 1000 Ljubljana, Slovenia

ARTICLE INFO

Article history:
Received 23 January 2011
Received in revised form 11 April 2011
Accepted 11 April 2011
Available online 20 April 2011

Keywords:
Ce modification in A360 alloy
Reaction kinetics
Mechanical properties
Differential scanning calorimetry

ABSTRACT

The effect of Ce addition on the AA A360 (Al–10%Si–0.5%Mg) alloy was investigated using equilibrium thermodynamic calculation, thermal analysis, differential scanning calorimetry (DSC) and scanning electron microscopy (SEM). The purpose is to study the variations that occur during solidification and precipitation with different Ce additions, as well as their effect on the mechanical properties. The results show that the Ce addition decreases the eutectic ($\alpha_{Al} + Mg_2Si$) temperature. The solidus temperature also decreases with the increasing Ce addition. The precipitation enthalpy determined using DSC decreases with the Ce addition, while precipitation takes place more rapidly and intensively, indicating increased reaction kinetics. The mechanical properties like hardness and tensile strength also increase with the Ce addition. The phase that contributed to the hardness of the investigated alloy was composed of Al, Ce, Mg and Si.

1. Introduction

Aluminium–silicon casting alloys have numerous applications in the automotive industry because of a specific feature involving high strength-to-weight ratio, thereby increasing mechanical performance and decreasing fuel consumption in vehicles. 6xxx series Al–Si–Mg alloys (EN standard) are widely used alloys for automobile die-casting industry. It is used for thin-wall castings [1] in automobile, aircraft and chemical industry. Mg addition to the binary Al–Si alloy enables heat treatment [2,3], and consequently the increase of the mechanical properties [4–8].

Rare earth metals, such as cerium (Ce), have been found to improve the mechanical properties of Al–Si castings through modifying their microstructure and enhancing the tensile strength [9] and ductility [10], heat resistance and extrusion behaviour [11]. The solidification of Al–Si alloys with Ce addition can be described by ternary phase diagram in Fig. 1. [12], which unfortunately does not include other alloying elements and other multicomponent phases with Ce. It was reported that these Ce-phases may act as nucleation sites for (Al) or (Si) crystals in both hypo- and hypereutectic Al–Si alloys [13]. The solidification sequence of such investigated alloy is following: primary crystals of α_{Al} together with $Al_{15}(FeMn)_3Si_2$ phase, eutectic ($\alpha_{Al} + \beta_{Si}$) together with AlFeSi-β phase, eutectic ($\alpha_{Al} + Mg_2Si$) and eutectic ($\alpha_{Al} + Al_5Mg_8Si_6Cu_2$) [4], at the end of the solidification also Ce-rich phase solidify.

The influence of Ce on ternary Al–Si–Mg alloys was not investigated yet. This investigation represents great importance from this reason that this ternary A360 alloy presents the basics for the commercial Al–Si–Mg alloys.

2. Experimental

A commercial A360 alloy was melted in an electric induction furnace, and various concentrations of pure (99.9%) Ce (0, 0.01, 0.02, 0.05 and 0.1 wt.%) were added. Chemical composition of the investigated samples is presented in Table 1. Based on the obtained chemical compositions of the alloys (Table 1) the equilibrium solidification and equilibrium phase diagrams (Fig. 2) were simulated with Thermo-Calc program TCW 5 and database COST507. Mass fraction of the phases regarding the Ce addition was calculated. After the basic alloy was melted, the Ce was added into the melt. After 10 min the melt was poured into a measuring cell with a controlled cooling system (simple thermal analysis – STA) with the purpose to record cooling curves at different cooling rates. Simultaneously, the specimens for the tensile tests were also cast into a mould made according to standard DIN50125. The characteristic solidification temperatures were determined from the cooling curves, and the influence of Ce was defined. Furthermore the samples for DSC and microstructure analysis were taken from the specimens after STA. The DSC instrument (Jupiter 449c, NETZSCH) was calibrated and the basic curve was recorded. The measurements were carried out after 7–10 days after casting into STA under a protective Ar-atmosphere by following temperature program: heating rate 10 °C/min up to 710 °C → holding at 710 °C for 10 min → cooling rate 10 °C/min. Moreover DSC curves were plotted, temperatures of the precipitation were marked and the formation enthalpies of precipitates were determined. The precipitate fraction regarding temperature and the intensity of the precipitation was determined. In addition the specimens were examined using a scanning electron microscope (SEM) SIRION 400nc, FEI Company equipped with an EDS analyzer INCA 350. Cerium phase was identified. Hardness was measured using universal Brinell hardness tester and the tensile strength was defined on as cast specimens made according to standard DIN50125 using Simulator of thermomechanical states GLEEBLE 1500D.

* Corresponding author. Tel.: +386 12000418; fax: +386 14704560.
E-mail address: maja.voncina@omm.ntf.uni-lj.si (M. Vončina).

0925-8388/$ – see front matter © 2011 Elsevier B.V. All rights reserved.
doi:10.1016/j.jallcom.2011.04.059

Table 1
The chemical composition of investigated Al–Si–Mg alloy.

Alloy	Element/wt.%							
	Si	Mg	Mn	Cu	Ti	Fe	Ce	Al
AlSi10Mg	10.75	0.39	0.26	0.04	0.02	0.53	0	Rest
AlSi10Mg + 0.01 Ce	10.61	0.39	0.27	0.04	0.02	0.59	0.009	Rest
AlSi10Mg + 0.02 Ce	10.67	0.38	0.30	0.04	0.02	0.60	0.016	Rest
AlSi10Mg + 0.05 Ce	10.37	0.37	0.29	0.04	0.03	0.66	0.047	Rest
AlSi10Mg + 0.1Ce	10.78	0.40	0.29	0.04	0.02	0.61	0.097	Rest

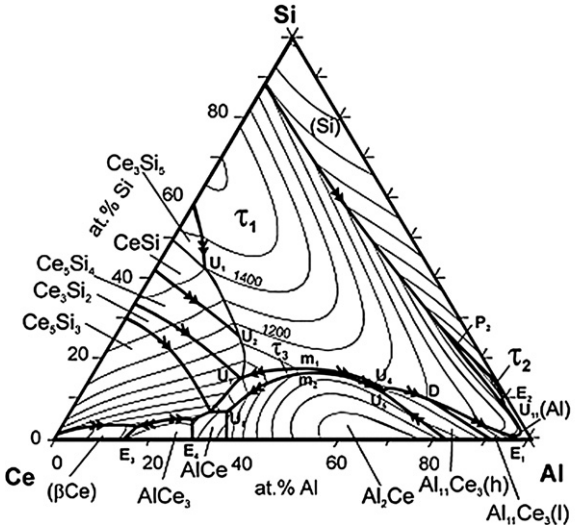

Fig. 1. Liquidus surface of ternary system Al–Si–Ce [12].

3. Results and discussion

3.1. Effect of Ce on the equilibrium solidification

Fig. 2 shows the calculated equilibrium vertical cross section diagram at 0.02 wt.% Ce. Here the solidification starts with formation of Si_2Ti phase. Next phases formed during solidification are crystals of α_{Al} and AlFeSi-β phase. Upon further cooling the phase AlMnSi-α (presumably $Al_{15}(FeMn)_3Si_2$) precipitates followed by the binary eutectic reaction ($\alpha_{Al} + \beta_{Si}$) at 573 °C. At line 15 that presents liquid the solidification ends and this is the solidus temperature. Moreover the Mg_2Si phase precipitates from the solid solution at around 510 °C and Al_2Cu phase at around 160 °C. Database COST507 indicates that Ce phase solidifies at around 560 °C as Al_8Ce phase. This database in incomplete and it should be complemented with multicomponent Ce phases. Fig. 3 shows the calculated mass fraction of phases at temperature 298 °C in dependence of Ce-addition. The increasing Ce-content in the alloy reduces the mass fractions of α_{Al} and β_{Si} phases, and consequently eutectic ($\alpha_{Al} + \beta_{Si}$). Mass fraction of Mg_2Si slightly reduces with increasing Ce addition and mass fraction of Al_8Ce phase increases as the concentration of Ce increases.

3.2. Effect of Ce on the solidification

Fig. 4 shows a typical cooling curve together with a differential cooling curve of A360 alloy. The characteristic solidification temperatures were determined in all specimens with various Ce additions (Table 2). Striped line indicates the theoretical, with the Thermo-Calc calculated, liquidus temperature for these alloys. The liquidus temperature (Eq. (1)) was modelled using multiple regression method in Origin 7.0 program:

$$T_L = 660,39286 - 6.7\%\mathrm{Si} - 2.5\%\mathrm{Mg}\,\partial y \quad (1)$$

Dotted line in Fig. 4 indicates theoretical calculated eutectic temperature (Eq. (2)) of this alloy:

$$T_E = 573,82143 + 0.2\%\mathrm{Si} - 2.5\%\mathrm{Mn} - 5\%\mathrm{Mg} \quad (2)$$

The main difference in comparison to Ce-free alloy on the cooling curve occurred at the temperature of eutectic solidification T_{E2} ($\alpha_{Al} + Mg_2Si$) where the temperature decreased with the increasing Ce addition in the alloy (Table 3). The same tendency was observed on the heating and cooling DSC curves (Fig. 5). The eutectic temperature for the ($\alpha_{Al} + Mg_2Si$)-eutectic decreased when Ce was added (Table 3).

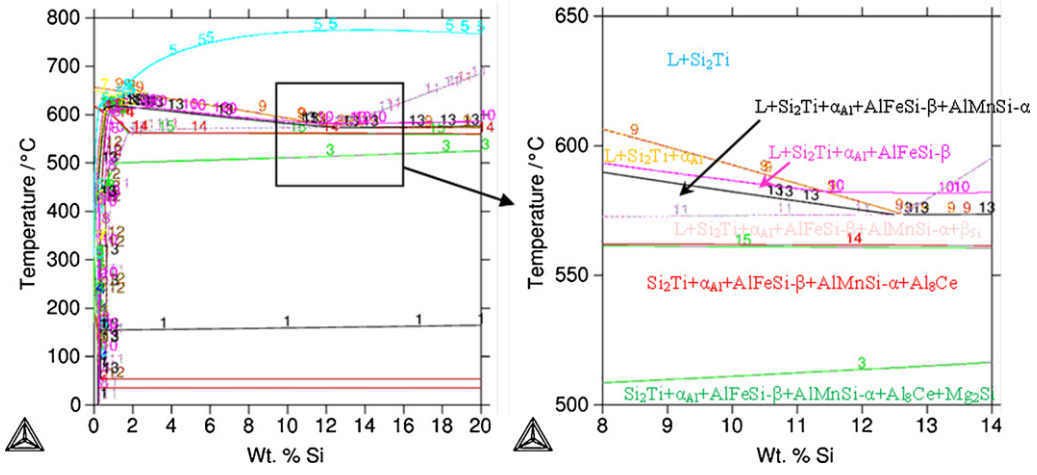

Fig. 2. Isoplete equilibrium phase diagram of A360 with 0.02 mass% Ce.

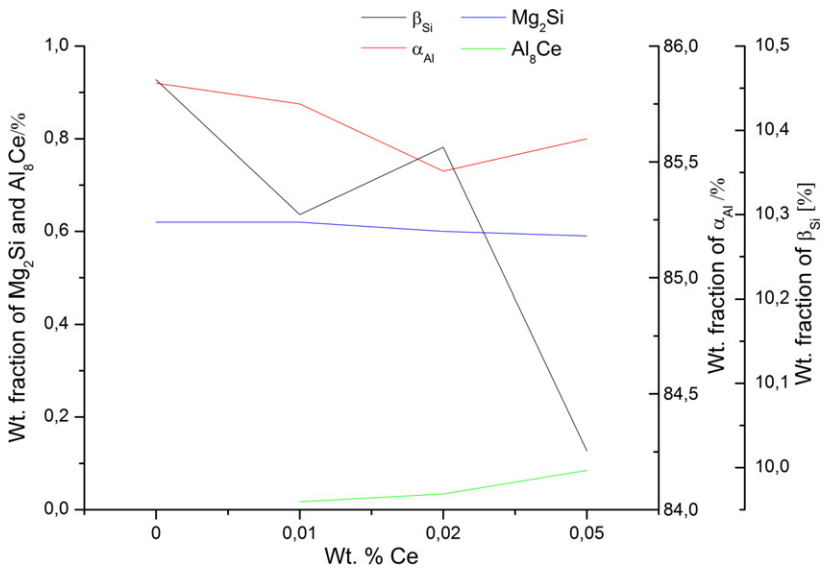

Fig. 3. Calculated weight fraction of phases in dependence of Ce addition in A360 alloy at 298 °C.

Table 2
Characteristic temperatures of solidification of A360 alloy from STA.

Mass% Ce	$T_{Ltheor.}$/°C	$T_{L/min}$/°C	$T_{L/max}$/°C	$\Delta T_{Lp.}$/°C	$\Delta T_{Lr.}$/°C
0	587.4	579.6	581.5	7.8	1.9
0.01	588.3	580.5	584.5	7.8	4
0.02	587.9	578.2	582.5	9.7	4.3
0.05	590	580.8	584	9.2	3.2

Mass% Ce	$T_{Etheor.}$/°C	$T_{E/min}$/°C	$T_{E/max}$/°C	$\Delta T_{Ep.}$/°C	$\Delta T_{Er.}$/°C	$T_{E2(Mg2Si)}$/°C	$T_{E3(AlFeMnSi)}$/°C	T_S/°C
0	573.4	562.5	566.5	10.9	4	551	547.5	536.5
0.01	573.3	565.3	567.9	8	2.6	550.5	547.8	538.3
0.02	573.3	564	567.5	9.3	3.5	548.5	547.6	534.9
0.05	573.3	565.6	568.1	7.7	2.5	547.5	546.5	535.5

3.3. *Effect of Ce on the precipitation of Mg_2Si precipitates*

The addition of Ce and cooling rate also influences on the precipitation of Mg_2Si phase that occurs at around 210 °C (Fig. 6a). When specimens were cooled with cooling rate of 10 K/min, the precipitation occurs at 212.9 °C in the Ce-free alloy, whilst the precipitation temperature is reduced to 212.2 °C, 207.9 °C and 202.3 °C when 0.02 wt.% Ce, 0.05 wt.% Ce and 0.1 wt.% Ce is added to the alloy, respectively. The precipitation enthalpy also decreases with increasing Ce addition and increases with the increasing cooling rate at STA (Fig. 6b). It was anticipated that Ce in A360 alloy decreases the activation energy for the precipitation of Mg_2Si phase and consequently precipitation enthalpy.

Fig. 7a clearly shows that Ce also influences the precipitation intensity. When Ce is added the precipitation takes course faster than at pure alloy. Optimal concentration of Ce in the alloy accelerates precipitation of Mg_2Si phase. Faster cooling rates prevent diffusion of Mg out of the solid solution, consequently, during reheating the precipitation is more intense (Fig. 7b). The slope of the transformation curve increases as the precipitation kinetics increases.

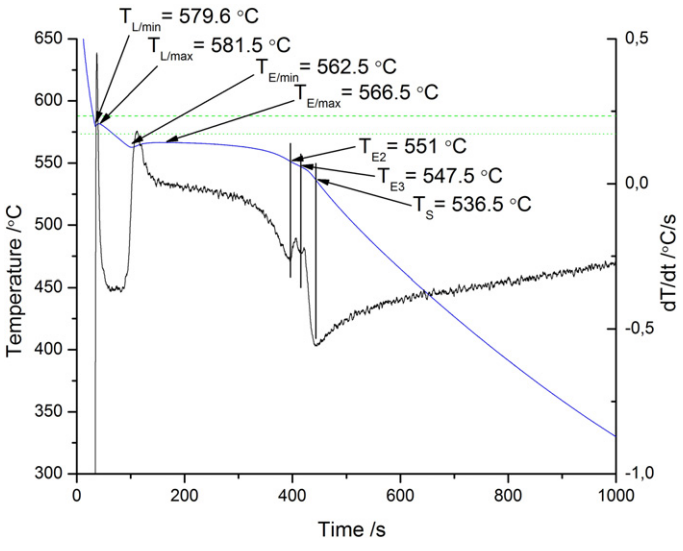

Fig. 4. Cooling curve and differential cooling curve of A360 alloy with indicated theoretical calculated equilibrium liquidus and eutectic temperature (horizontal line).

Table 3
Eutectic temperature for (α_{Al} + Mg_2Si) determined using STA and DSC.

Wt.% Ce	$T_{E2(Mg2Si)}$/°C	
	STA	DSC
0	551.0	553.2
0.01	550.5	549.8
0.02	548.5	549.4
0.05	547.5	549.7

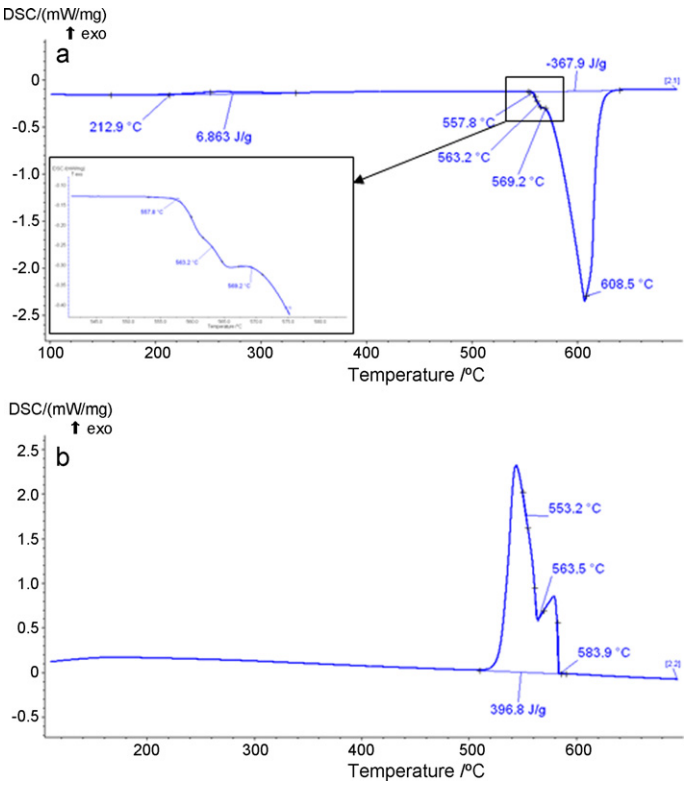

Fig. 5. Heating (a) and cooling (b) DSC curve of A360 alloy.

3.4. Effect of Ce on the microstructure

Figs. 8 and 9 show SEM micrographs of A360 alloy with Ce. In the microstructure all the standard microstructure elements characteristic for this type of the alloy were found: primary crystals of α_{Al}, eutectics ($\alpha_{Al} + \beta_{Si}$) and ($\alpha_{Al} + Mg_2Si$) and also AlFeSi (presumably Al_5FeSi-β) and AlFeMnSi (presumably $Al_{15}(FeMn)_3Si_2$)phase. Ce formed intermetallic compound combined of Al, Ce, Mg and Si that solidifies in rounded polyhedral shape (Fig. 8). The composition of Ce-rich phase is close to Al_2CeSi_2. This may correspond to presumably a metastable τ_4 phase found in Ref. [12]. When the specimens were deeply etched [14] the precipitates Mg_2Si were also detected (Fig. 9).

3.5. Effect of Ce on the mechanical properties

Tensile strength increases from 212 N/mm^2 up to 245 N/mm^2 at 0.01 wt.% Ce where it reaches maximum and decreases down to 218 N/mm^2 at 0.02 wt.% Ce and to 225 N/mm^2 at 0.05 wt.% Ce (Fig. 10). When suitable concentration of Ce is added the alloy reaches the same tensile strength as it was heat treated, so the additional treatment is not necessary.

The Brinell hardness was tested on all investigated specimens after STA. Results are shown in Table 4 and Fig. 11. The hardness of A360 alloy is improved when suitable concentration of Ce is added and at higher cooling rates. As it was reported [10], Ce-phases act as a barrier for dislocation moving and in this way increase the mechanical properties.

Ce-phase in A360 alloy occurred in rounded polyhedral. Authors that investigated Al–Si–Ce system [11–13], described the solidification of τ_1 ($Ce(Si_{1-x}Al_x)_2$), τ_2 ($AlCeSi_2$), τ_3 (Al_xCeSi_{2-x}) and

Table 4
Tensile strength and Brinell hardness.

Wt.% Ce	Tensile strength/MPa	Brinell hardness/HB		
		10 K/min	100 K/min	300 K/min
0	212	57.7	67.5	77.9
0.01	245	63.6	67.5	83
0.02	218	54.8	70.2	73
0.05	225	59	59	84.9

τ_4 (Al_2CeSi_2) phases. In this investigated alloy with 10 wt.% Si only τ_2 phase could occur, which solidifies as a ternary eutectic ($\tau_2 + \alpha_{Al} + \beta_{Si}$). The solubility of Ce in Al is <0.01at.% at room temperature. The reason for low solubility can be found in big difference in atomic radius; for Ce is 1.81 Å, for Al is 1.41 Å. For this reason Ce in these alloys forms intermetallic compounds [15]. Similar was found when the influence of alkaline earth metal Ba in Al–Si–Mg alloy was investigated. Ba increased the mechanical properties, but only when suitable concentration of Ba in the alloy was added [16].

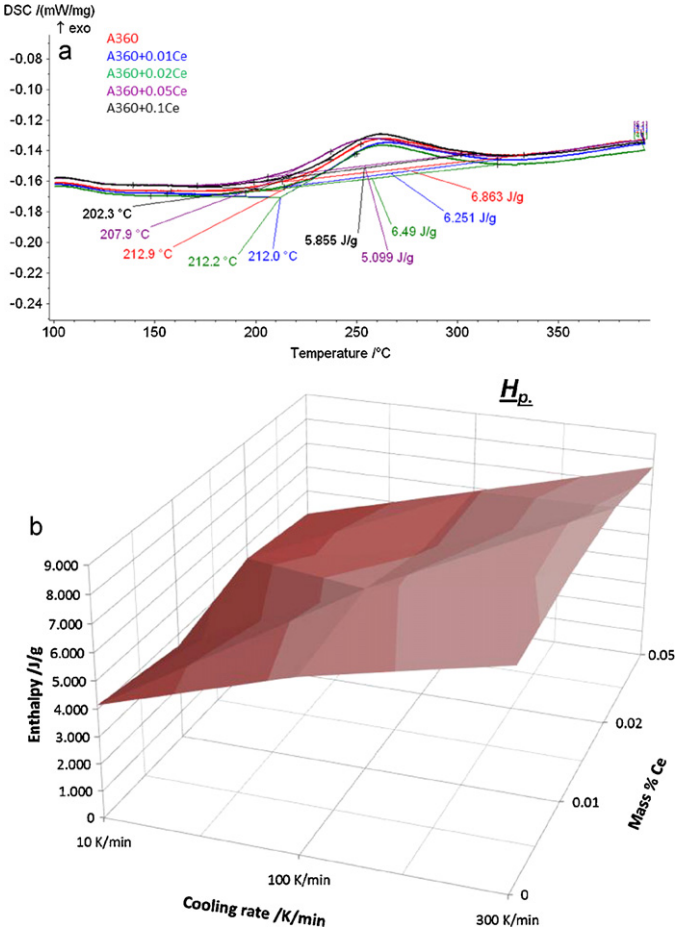

Fig. 6. Comparison of precipitation temperature regarding the Ce addition (a) and precipitation enthalpy regarding the Ce addition and cooling rate at heating DSC curves (b).

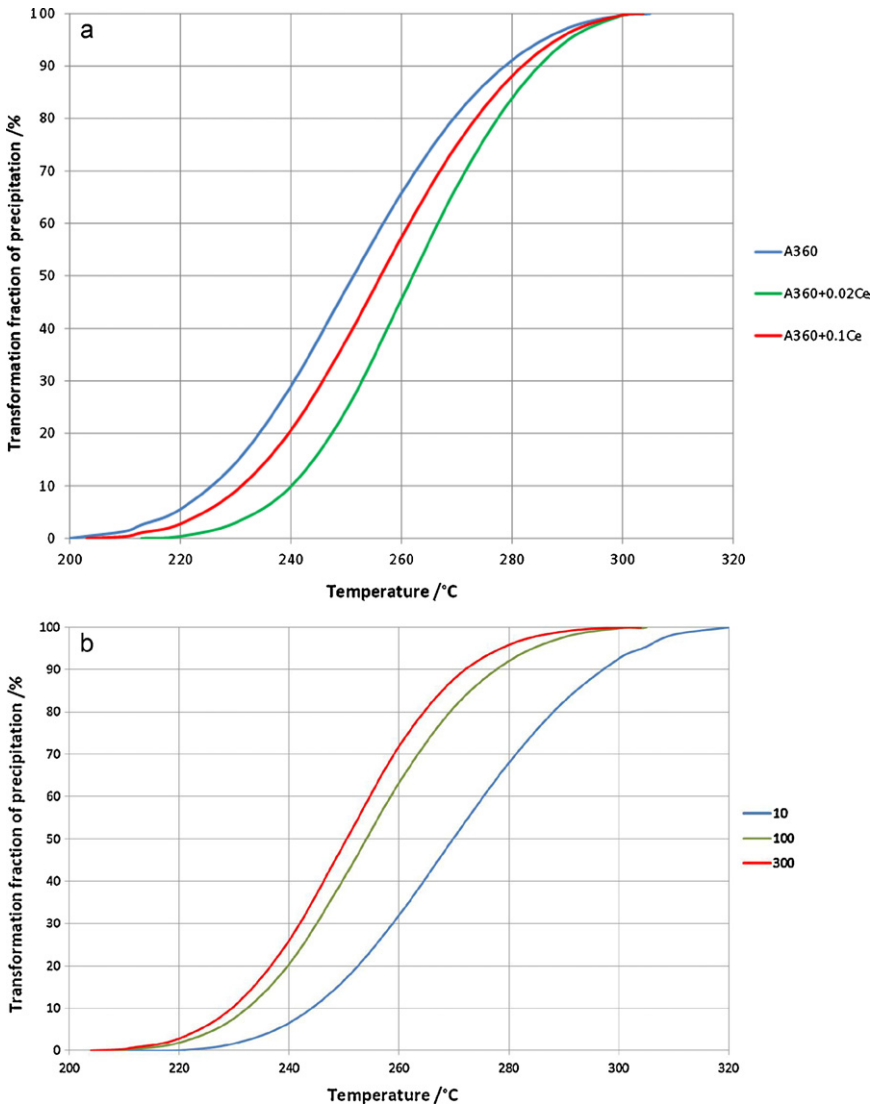

Fig. 7. Fraction of precipitation transformation regarding Ce addition (a) and regarding cooling rate (b).

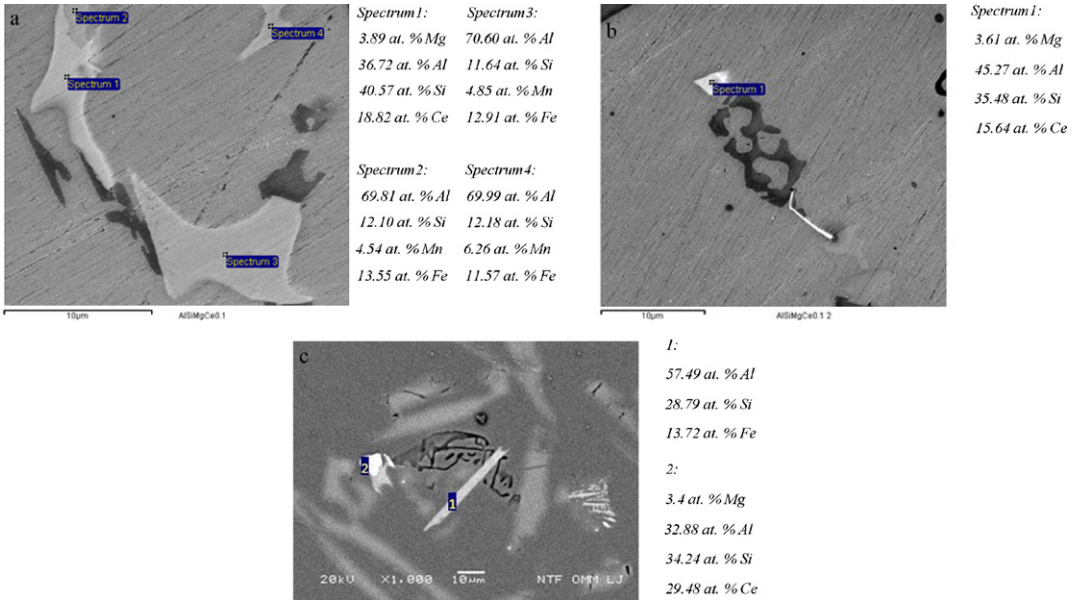

Fig. 8. SEM micrograph of specimen A360 with 0.01 wt.% Ce from STA: Ce-phase (Spectrum 1), AlFeMnSi (Spectrum 2), AlFeMnSi (Spectrum 3), AlFeMnSi (Spectrum 4) (a), Ce-phase (b) and AlFeSi (1) and Ce-phase (2) (c).

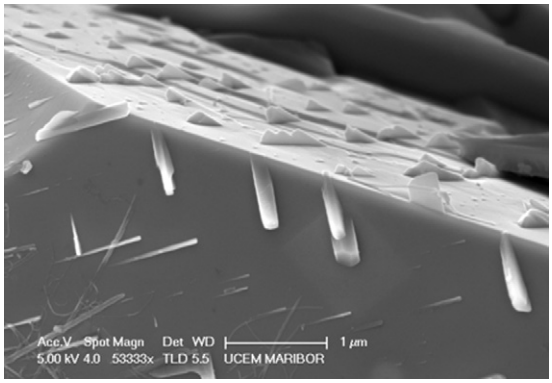

Fig. 9. Deeply etched specimen from A360 + 0.02 wt.% Ce from STA.

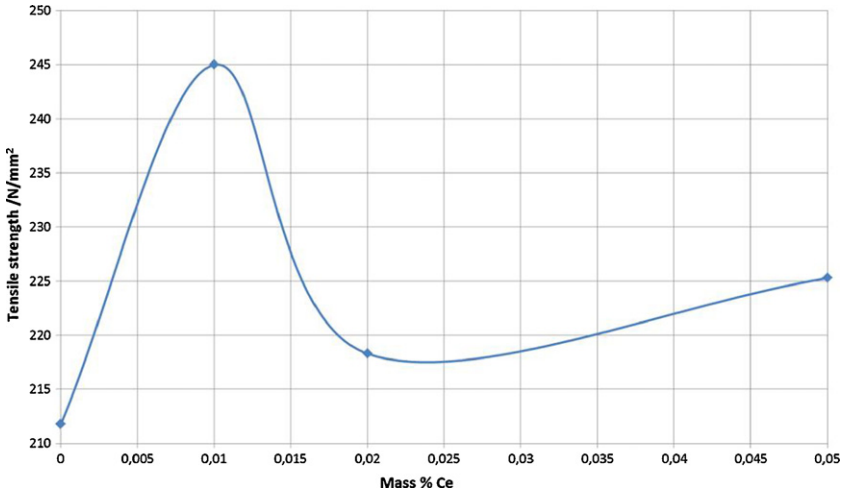

Fig. 10. Tensile strength of A360 alloy with various Ce additions.

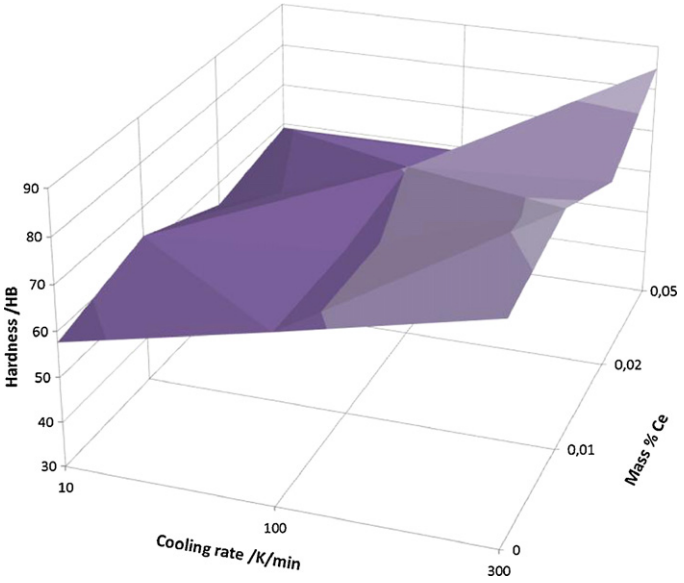

Fig. 11. Brinell hardness of A360 alloy regarding Ce addition and cooling rate.

4. Conclusions

The effect of Ce and cooling rate on the solidification and precipitation were investigated. Furthermore, tensile strength and Brinell hardness of modified A360 alloy were analysed.

1. When the equilibrium calculation is considered, wt.% of Mg_2Si slightly reduces with increasing Ce addition. Wt.% of Ce-phase increases as the concentration of Ce increases. Database COST507 in Thermo-Calc program have some deficiency: they should be complemented with multicomponent phases with Ce.
2. The solidification of eutectic ($\alpha_{Al} + Mg_2Si$) shifts to lower temperature when Ce is added.
3. Ce influences on the precipitation temperature and it is decreasing with the increasing concentration of Ce. The precipitation enthalpy also decreases with increasing Ce addition. When Ce is added the precipitation kinetics is faster. Addition Ce in the alloy and higher cooling rate accelerates the precipitation kinetics.
4. Rare earth metals such as Ce have been found to improve the mechanical properties of Al–Si castings where they modify the microstructure and enhance the tensile strength and hardness when Ce is added. Phase that enhanced the hardness was found to be quaternary intermetallic phase composed of Al, Ce, Mg and Si.

Acknowledgements

The authors would like to thank to Dr. Franc Zupanič, University of Maribor, Faculty of Mechanical Engineering and to Dr. Aleš Nagode, University of Ljubljana, Faculty of Natural Sciences and Engineering for work on SEM.

References

[1] ASM Metals Hand Book, vol. 15, Casting, Published in 1988.

[2] G. Terjesen, Aluminium 79 (9) (2003) 748–754.
[3] B.K. Shah, S.D. Kumar, D.K. Dwivedi, Materials and Design 28 (2007) 1968–1974.
[4] L. Bäckerud, G. Chai, J. Tamminen, Solidification Characteristics of Aluminum Alloys, vol. 2, Foundry Alloys. AFS/SKANALUMINIUM. Department of Structural Chemistry – Arrhenius Laboratory, University of Stockholm, 1990.
[5] S. Esmaeili, D.J. Lloyd, W.J. Poole, Acta Materialia 51 (2003) 3467–3481.
[6] S. Esmaeili, D.J. Lloyd, Acta Materialia 53 (2005) 5257–5271.
[7] Q.G. Wang, C.J. Davidson, Journal of Material Science 36 (2001) 739–750.
[8] C. Vorge, M. Jucgues, M.P. Schmidt. Corrosion of Aluminium, 2001.
[9] M. Vončina, S. Kores, J. Medved, Influence of Ce addition on the solidification and mechanical properties of AlSi10Mg alloy, Tofa 2010 discussion meeting on Thermodynamics of AF, Book of abstracts and Programme, Faculdade de Engenharia da Universidade do Porto, Portugal, 2010, p. 75.
[10] H.R. Ammar, C. Moreau, A.M. Samuel, F.H. Samuel, H.W. Doty, Materials Science and Engineering A 489 (1–2) (2008) 426–438.
[11] Y. Wu, J. Xiong, X. Renming Lai, Z. Zhang, Guo, Journal of Alloys and Compounds 475 (1–2) (2009) 332–338.
[12] V. Raghavan, Journal of Phase Equilibria and Diffusion 28 (5) (2007) 456–458.
[13] J. Gröbner, D. Mirkoviĭc, R. Schmid-Fetzer, Metallurgical and Materials Transactions A 35A (November 2004) 3349–3362.
[14] T. Bončina, B. Markoli, I. Anžel, F. Zupanič, Zeitschrift Fur Kristallographie 223 (2008) 747–750.
[15] H. Yia, D. Zhanga, T. Sakatab, H. Morib, Journal of Alloys and Compounds 354 (2003) 159–164.
[16] X.H. Zhang, G.C. Su, C.W. Ju, W.C. Wang, W.L. Yan, Materials and Design 31 (2010) 4408–4413.